MEASUREMENTS OF PRESSURE IN A SQUEEZE FILM DAMPER WITH AN AIR/OIL BUBBLY MIXTURE

by

Luis San Andrés

April 1996

TRC-SFD-1-96

Texas A&M University
Mechanical Engineering Department

Measurements of Pressure in a Squeeze Film Damper With an Air/Oil Bubbly Mixture

by

Sergio Diaz
Ph. D. graduate student

A Research Progress Report
to the
Turbomachinery Research Consortium

Subject: Squeeze Film Dampers

May 1996

TRC Project:
Experimental Study of the Response of Squeeze Film Damper Supported Rotors.
Principal Investigator: Dr. Luis San Andres, Associate Professor

Measurements of pressure in a squeeze film damper with an air/oil bubbly mixture

Abstract

An insight on the effects of air ingestion on the performance of squeeze film dampers (SFDs) is presented. A test rig consisting on a circular centered orbit squeeze film damper fed with a bubbly mixture of oil and air is used. Measurements of the dynamic pressure field at a fixed speed and with different air/oil volume ratios are obtained. The measurements allow to establish some trends on the behavior of the peak to peak dynamic pressure developed on the film and the power required to drive the damper when the amount of air present in the fluid film is varied. The pressure fields are analyzed for consecutive cycles of journal motion to capture the effect of the variations on the amount of air present in the lubricant. The tests show the dynamic pressure generation in the squeeze film decreases when the air/oil volume ratio is increased. When the air amount in the lubricant is large enough, there occurs a zone of no pressure variation referred to as gas cavitation. It is not a stable phenomenon, varying from one cycle of journal motion to another. There is even a transition zone in which, for certain amounts of air in the mixture, this zone appears only in some of the journal motion cycles. Measurements of the driving power on the SFD journal shaft were also taken and showed a trend to decrease with increments on the air/oil ratio, and giving some evidence of lubricant mixture viscosity reduction.

Table of Contents

Introduction

The two most commonly recurring problems in rotordynamics are excessive steady-state state synchronous vibration levels, and subharmonic rotor instabilities. Squeeze film dampers (SFDs) have been successfully used to solve these problems, stabilizing otherwise unstable units (Childs, 1993). Although SFDs are widely used in modern high speed turbomachinery, their operation is yet not fully understood (Walton et al. 1987).

As with journal bearings, the incompressible-fluid Reynolds equation is generally used to model squeeze film dampers. However, because of dynamic lubricant cavitation phenomena, the correlation between theory and experiment is considerably less compelling for dampers than bearings (Childs, 1993, Walton et al., 1987, and Zeidan and Vance, 1989). In particular, the presence and extent of cavitation or film rupture and its effects on damper performance are difficult to predict. There is a lack of physical understanding of the phenomena of dynamic film rupture. Several authors have reported the occurrence of two different mechanisms of cavitation in squeeze film dampers, namely, vapor cavitation and gaseous cavitation (Hibner and Bansal 1979, Zeidan and Vance 1989, Walton et al. 1987).

Vapor cavitation occurs in an isothermal process when the fluid pressure drops to its saturation value and a phase change (vaporization) follows. Gaseous cavitation occurs when the relative movement between the two parts of the damper drags air into the film or releases air dissolved in the oil leading to a two phase lubricant mixture. This last mechanism is the most commonly found in commercial applications of squeeze film dampers. To this date there is no accurate model for predicting gaseous cavitation effects on SFD performance.

Zeidan and Vance (1989) and Walton et al. (1987) have made observations of SFD film flows with high speed motion pictures, and found that the occurrence of gaseous cavitation leads to a two phase mixture within the film. The air present in the mixture forms bubbles, persisting even in the high pressure zone. In this way, the squeeze film damper becomes to be lubricated with a **bubbly mixture** of oil and air.

The oil-air bubbly mixture is certainly non homogeneous within the film. Undaunted by the complexity, Chamniprasart et al. (1993) have addressed to the importance of air entrainment on bearing performance. These authors developed a model for determining the pressure field on a squeeze film damper lubricated with binary mixtures, in particular a bubbly oil. The model assumes the lubricant to be a mixture of a Newtonian liquid (oil) and an ideal gas (air). Using mixture theory the Reynolds equation is modified to account for a multi-phase continua. Another way to include the presence of air in the lubricant could be to estimate an effective viscosity. However, the available models (Einstein, 1906, Taylor, 1932, and Hayward, 1961) were developed for conditions in which the shear

force in the fluid remains small in comparison with the surface tension acting on the oil-air interfaces. These models predict an increment on the viscosity when small amounts of air are present. However, it is suspected that these models will not be valid under typical lubrication conditions in SFDs, where the small clearances cause shear stresses to be the most important factor, and the bubbles can be very large in comparison to the film thickness.

Experimental Facility

The experimental apparatus is shown in Figure 1a. The test section consists of a journal (L=2.4 cm, D=12.7 cm) mounted on an eccentric sleeve with a ball bearing to provide a controlled circular orbit. The eccentric is mounted on a rigid shaft in an overhung configuration, driven by a variable speed electrical motor through a toothed belt. The journal has four antirotation "ears" that allows it to whirl but not to spin. The whirl frequency (equal to shaft speed) is measured by an optical sensor. The nominal radial clearance (C) of the damper is 0.343 mm (13.5 mils) and the nominal eccentricity (e) is 0.216 mm (8.5 mils).

The oil employed on the tests is an ISO VG 68 of density equal to 0.87 g/cm^3, and viscosity equal to 77.5 cPoise at 28 °C and 25.8 cPoise at 50.9 °C. The viscosity values were determined experimentally using a Model RI:1:L viscometer manufactured by Rheology International. The oil is stored in a 113.6 liters (30 gallons) reservoir and delivered to the SFD test section via a gear pump (1800 RPM, 9.44 Liters/min., max. 2500 PSI, 0.2 KW). The damper is lubricated with a bubbly mixture of oil and air, and the amount of air in the mixture can be controlled by adjusting the air flow through a sparger element. A sketch of the lubricant and air feeding system is depicted in Figure 2.

The flow rates of oil and air are regulated by setting the valves in the oil line, air line, and oil bypass. The mixture is produced at the sparger (mixer element) in the junction of both lines. The static feeding pressures of oil and air are read in the pressure gauges PG_1 and PG_2, respectively. An additional gauge (PG_3) allows to register the pressure of the air oil mixture just before its entrance to the damper test section. To establish qualitatively the condition of the mixture, there are two windows, made of transparent hoses, located at the inlet and outlet ports of the SFD. The lubricant inlet and outlet temperatures, the film temperature, and the air supply temperature, are measured with K-type thermocouples (TT).

The lubricant is feed to the damper left end through two holes, one at the top and one at the bottom. This left end is sealed with an O-ring so there is no leakage in this direction (see Figure 1b). The right end is open, allowing all the flow to go this way and maximizing the axial pressure variation.

The motion of the journal is registered with two non-contact eddy current sensors (PP_X and PP_Y) orthogonally located at the axial location Z_3 (3.71 cm from the left end). On the horizontal plane, where PP_X is located, there are two

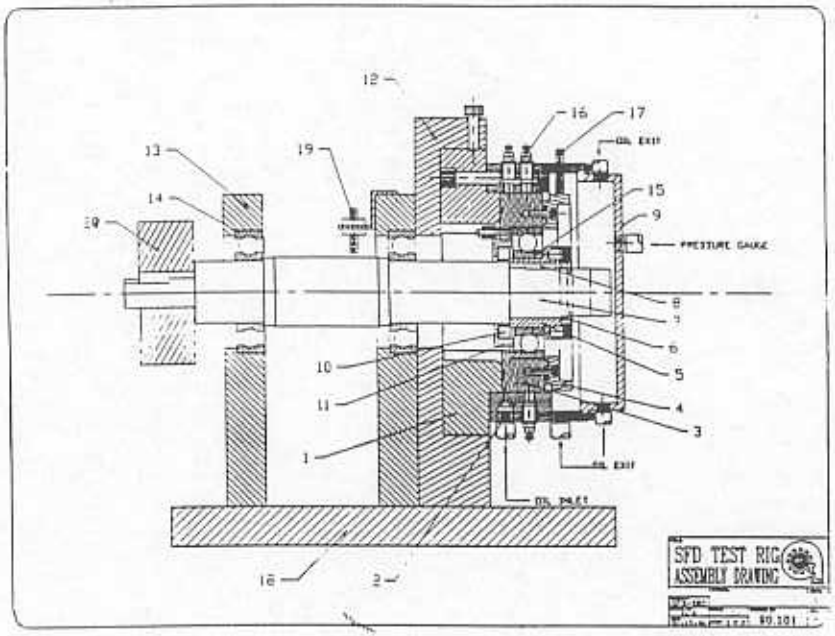

REFERENCES

1.- HOUSING END PLATE
2.- HOUSING
3.- JOURNAL
4.- END PLATE
5.- ECCENTRIC
6.- ECCENTRIC HOLDER
7.- SHAFT
8.- KEY
9.- HOUSING CAP
10.- LIP SEAL
11.- LEFT SEAL PLATE
12.- HOUSING SUPPORT
13.- SHAFT SUPPORT
14.- SHAFT BEARINGS
15.- JOURNAL BEARING
16.- PRESSURE NUTS
17.- PROXIMITY PROBE
18.- BASE PLATE
19.- OPTICAL SPEED SENSOR
20.- TRANSMISSION WHEEL

(a) General Assembling

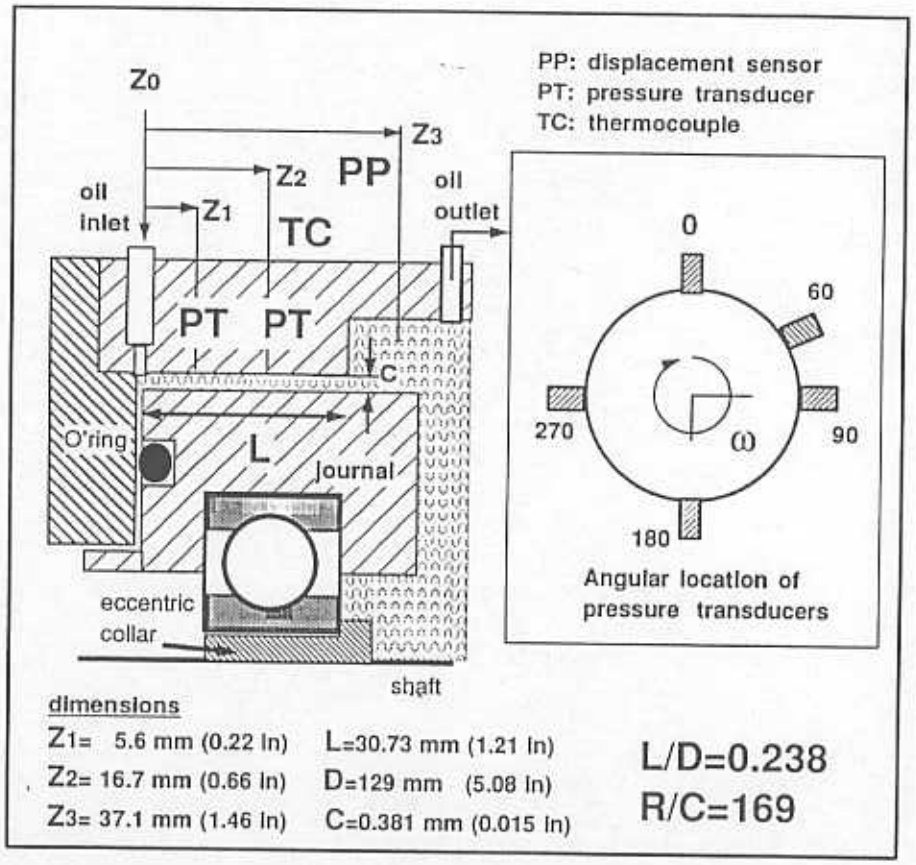

(b) SFD Detail

Figure 1.- SFD Test Apparatus

dynamic pressure transducers (PT_{Z1}, PT_{Z2}) installed at different axial positions. The location Z_1(0.56 cm from the left end) is nearer to the sealed end of the SFD, and Z_2(1.67 cm from the left end) is a location half way between Z_1 and the open end of the damper (see Figure 1b).

The signals of the pressure transducers and displacement sensors are monitored with oscilloscopes, conditioned with the aid of amplifiers, and recorded with an analog-digital board in a computer.

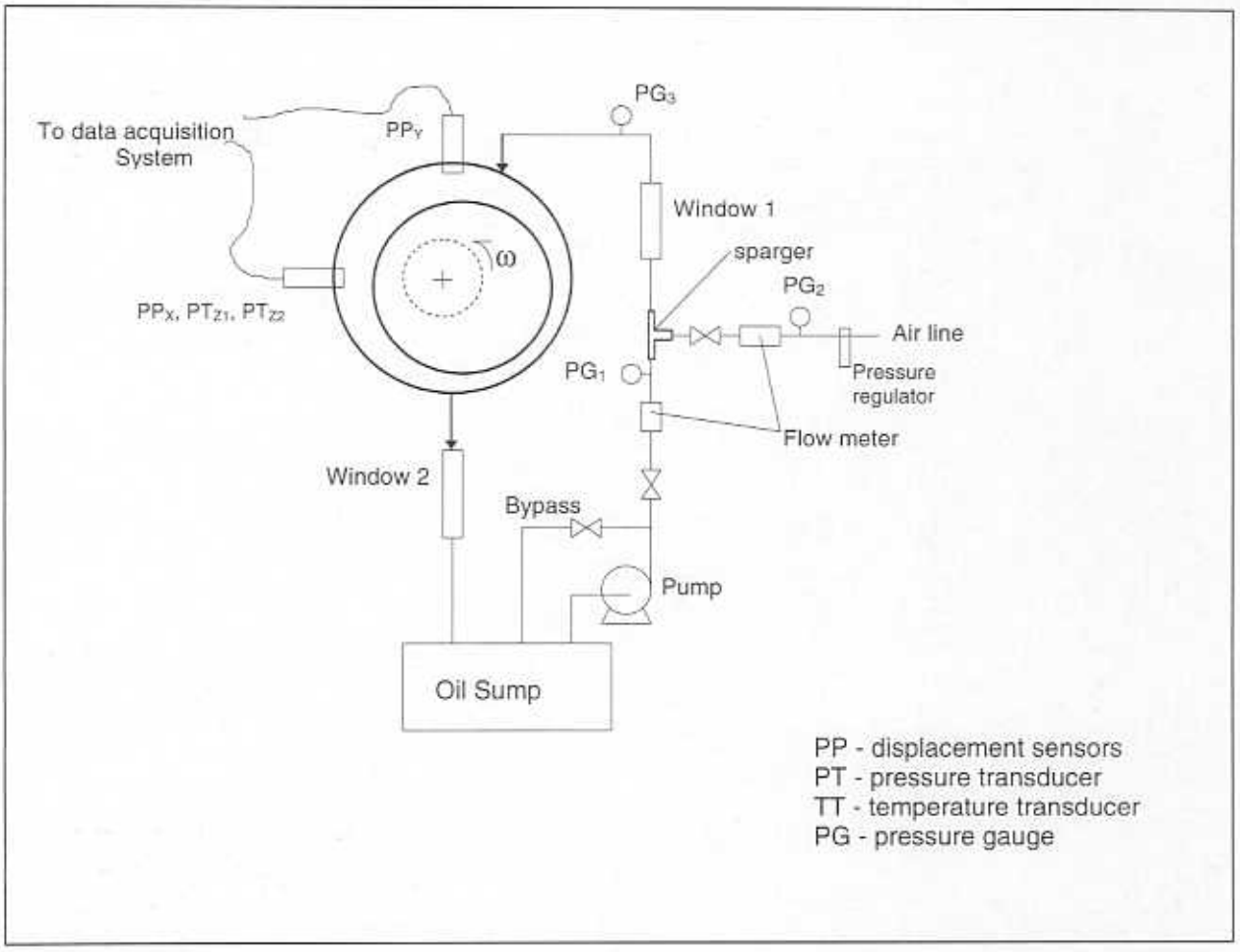

Fig. 2.- Sketch of Lubricant and Air Flow Lines

Experimental Procedure

To make evident the effect of the amount of air in the lubricant, all the other parameters of operation (speed, supply pressures, temperatures etc.) were set to fixed values. To this end, the shaft speed of was set to 1000 RPM (16.67 Hz). The valves on the oil lines were set to 3.1 bar (45 psi) of supply pressure (PG_1), and were maintained at the same position. The air pressure regulator was set to have a constant supply pressure of 2.7 bar (40 psi) in the air line (PG_2). There are several reasons that could allow to have mixture even when the oil pressure was higher than the air pressure. One possibility is that, because of a diameter reduction in the sparger, the oil is accelerated and its pressure could be locally decreased below that of the air allowing the mixture to occur. Of course, there is always the possibility that the pressure gauges were giving erroneous values. The air, oil, and mixture temperatures were kept constant with variations of less than $\pm 1°C$.

Several tests were conducted varying the air flow rate by setting the valve in the air line. For each test, the values of lubricant temperature, speed and feed pressures were recorded, as well as the voltage and current supplied to the electric motor. The time signals of the pressure transducers and displacement sensors were digitalized at a rate of 850 samples per second. With the digital data, the values of maximum and minimum film thickness and dynamic pressures, as well as the time records of each signal and the orbits of the journal center were obtained.

The air to oil volume ratio was established qualitatively by observation of the flow through the windows in the hoses. Thus, the values reported are not accurate, and can only be used as a relative reference to differentiate one condition to other within this study. Since there were no means to get quantitative measurements due to the smallness of the flow rates achieved, the values are given qualitatively based on visual observation as explained in the next section. The limitant to the oil flow rate was found to be an extremely high resistance across the piping.

Before taking measurements it was necessary to wait some time after setting the air valve to achieve a uniform mixture condition. The power supply of the motor needed to be reset to maintain a constant speed due to variations on the power consumption in the damper.

Results

Two sets of measurements were made to assure the repeatability of the data. They were made with one day of difference and found to show the same trends. Table 1 shows the results for the first set taken, and Table 2 for the second set. The tables present the values for all the parameters directly controlled in the experiment, as well as the values obtained after processing the data (dynamic pressures and film thickness).

It is necessary to explain the values given for Mixture Quality in Tables 1 and 2 before proceeding to the discussion of results. Due to a very high resistance in the oil feed line, the flows achieved for oil and air were too small to be registered with the flow meters available. The air to oil volume ratio values were assigned by observation of the lubricant through the inlet window (a 1/2" diameter transparent hose) giving a qualitative value for each studied condition. These values are used to provide a relative scale to differentiate one condition from others within this study, and may not represent effectively a ratio between air volume and oil volume flowing through the SFD. However, they can be used to establish a comparative scale to observe qualitatively the trends shown by the measurements.

The value of zero Mixture Quality is given to the test in which the lubricant is pure oil* , i.e. no air present. In this condition, both the inlet and the outlet windows showed no evidence of air. In the second case, a Mixture Quality of 10, the inlet window showed a pattern of very tiny bubbles (about 0.5 mm on diameter) plus a few small bubbles of about 5 mm in diameter flowing at a regular rate through the line, but very far away from each other (about 50 mm), see Figure 3a. The outgoing mixture showed a very similar pattern, but the tiny bubbles seemed to be more in quantity than in the inlet.

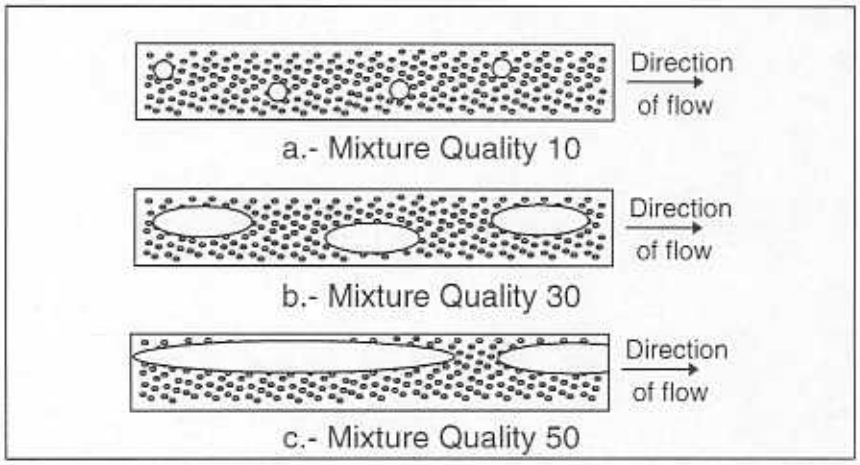

Fig. 3 - Flow patterns observed across inlet window

The condition named Mixture Quality 30 was one with a pattern very similar to the previous one, tiny bubbles uniformly distributed across the oil and midsize bubbles (30 mm length) about 30 mm from each other, see Fig. 3b. The outlet window showed a uniform foamy oil coming out from the SFD.

The condition of Mixture Quality 50 had a pattern of very large bubbles, which in occasions took almost half of the window, plus the tiny bubbles

* Note that most "pure" oil have at least 4 to 6% of air content.

uniformly distributed in the oil, see Figure 3c. The outlet window showed again a foamy oil pattern coming out from the damper.

For trend analysis purposes, it is proper to affirm that a larger value of Mixture Quality means more air within the film, giving a base for comparison. Figures 4 to 8 show the measurements taken at a lubricant mixture temperature of 28 °C and at a whirl speed of 1000 RPM (16.6 Hz). The top figures indicate the time variation of pressures at the locations Z_1 and Z_2 and the film thickness for several cycles of journal motion. Recall that the pressure and film thickness measurements are taken at the horizontal plane. The bottom figures depict the orbital pattern of the journal center motion for each of the tests.

Figure 4a shows the pressure profile for the case 1 of set #1 as a function of time. This condition (Mixture Quality 0) shows a typical behavior, with very similar pressure waves in the locations Z_1 and Z_2, but having higher values at Z_1. The pressure field shape agrees with those reported by Zeidan and Vance (1989) for SFD with vapor cavitation. The dynamic pressure varies as expected, being negative when the film thickness increases and positive when the journal is approaching the bearing. Note that journal motion in the X direction (film thickness) is at the same circumferential location as the pressure measurements. In this figure it can be seen that the film cavitates at the axial location Z_1 for a few seconds every cycle (a zone of constant pressure corresponding to a value close to zero absolute), while at Z_2 there is no evidence of cavitation. The pressure waves in this case are very stable and repetitive for every cycle of journal motion.

Figure 5a shows the pressure profile for the Mixture Quality 10, case 2 of set #1. Although the orbit radius has grown, the dynamic pressures are very similar to the ones of the previous case, but they have smaller amplitudes and are less stable in time. It can also be seen a small pressure perturbation right after finishing the cavitation region that fluctuates in time.

As the air/oil volume ratio is increased (see Figure 6a), there appears a zone in which the pressure stops increasing and remains more or less constant for a while (between points "a" and "b" of Figure 6a), and then begins increasing again. This phenomenon is described by Zeidan and Vance (1989) as gaseous cavitation. Figure 6a shows clearly that for the operating condition named Quality Mixture 30, this zone is unstable and does not appear in all the cycles. This condition seems to be a transition between the stable condition when there is no air and the very unstable condition shown in Figure 7a for Mixture Quality 50.

In the condition of Mixture Quality 50, case 4, Figure 7a, the pressure wave is very unstable, it presents the zone of no pressure increase (i.e. gas cavitation) in all cycles, but it is not repeatable in time (both, shape and size vary from one cycle to another). By observing the waves, it seems to be a condition in which there is free air enough to provide compressibility to the mixture and avoid

the pressure variation due to the squeeze effect. However, before the zone of no pressure variation, the pressure drops below this point for a while. It seems that when the film thickness is increasing (i.e. negative squeeze) the pressure decreases and the air-vapor bubbles increase in number and size until they collapse. At this point, depending on the amount of air or the size of the cavity that follows the bubbles collapse, the pressure sets to approximately the atmospheric pressure and remains more or less constant for the rest of the negative squeeze motion and part of the positive squeeze of the cycle. During this time, the work done by the motion is related to a volume variation of the lubricant instead of a pressure variation and that is why the dynamic pressures are smaller in this case. The first portion of the positive squeeze motion compresses the free air until the bubbles collapse or are expelled of the film. As the approaching motion continues the dynamic pressure increases until the positive squeeze finishes and then the pressure cycle is repeated.

Figures 4b to 7b provide information on the variation of the dimensionless orbit radius (e/c). The orbit radius is larger with larger amounts of air, and between the values of the case when there is no oil (Figure 8b) and when there is no air (Figure 4b). The test case of an SFD without oil (Figure 8) is included to provide some reference for the shape and size of the orbit, which is the same than for the static condition. The power required to drive the system in the absence of lubricant film is 352.8 Watts at 1,000 rpm.

Figures 4b to 7b also provide information about the fluctuation in the conditions where there is gas cavitation. It can be seen how in the condition of pure oil lubrication the orbit is very stable and repetitive during the five cycles represented. While when the air amount is increased the orbits become fluctuating and non repetitive for each cycle.

Figure 9, shows that the power required to drive the journal at constant speed is reduced when the air content is increased in the mixture. This can be explained because the air has lower viscosity than the oil, so the power required to drag the mixture within the squeeze film is lower. In both sets of measurements the data shows the same trend.

As it was discussed, the pressure waves are not stationary in time for the various cycles measured (see Figure 6a) and so are the peak-to-peak pressures. It was necessary to find an average value for the peak-to-peak pressure on each case. Figure 10 show the trend followed by the average peak-to-peak pressures at location Z2 for both sets of measurements. The average peak to peak pressure is shown to decrease with the amount of air in the damper. Figure 10 also shows the variations of the measured peak-to-peak pressure, including the maximum and minimum values for each case of set #1. Table 3 shows numerical values of this variation for the set #1 of measurements. For small amounts of air in the film, the pressure waves are almost stationary every cycle and the variations are small. When the air/oil ratio is increased, the variations are larger,

up to 8.77% above and 14.84% below the average value. This condition determines that, even when the average values are decreasing, the maximum peak to peak pressure increased from Mixture Quality 30 to Mixture Quality 50. That is, it was found at least one peak to peak pressure value for Mixture Quality 50 higher than the highest of Mixture Quality 30 and Mixture Quality 10.

Figure 11 shows the orbit radius to be affected by the presence of air in the lubricant. Though the journal is supposed to be rigid, tests made with pure oil and in the complete absence of oil, demonstrated that the dynamic pressure in the oil film produces a centering force large enough to produce appreciable variations on the dynamic eccentricity of the damper. The orbit radius increases when the air to oil ratio is augmented and approaches that of the no oil condition. This fact can be related to a decrement in the centering force, which is consistent with the reduction of the pressures. Figure 11 shows the average values of the dimensionless orbit radius (e/c) for each set of measurements. It also shows how the variations of the measured orbit radius in time also increased with the air/oil volume ratio for set #1.

It is known that the pressure in a squeeze film damper is proportional to the instantaneous eccentricity or orbit radius. For this reason it is introduced a parameter noted as Normalized peak-to-peak Pressure as the ratio of the peak-to-peak pressure to the dimensionless orbit radius. Figure 12, shows that if the orbit radius remains constant, the pressure keeps decreasing when the air volume in the mixture is increased. The points representing the variations for set #1 show that even the maximum peak-to-peak pressure follows this trend when normalized by the orbit radius.

Conclusions and Recommendations

An insight on the effect of air entrainment on the performance of squeeze film dampers is presented. A test rig consisting on a circular centered orbit squeeze film damper fed with a bubbly mixture of oil and air is used. Measurements of the dynamic pressure field at a fixed speed and with different air/oil volume ratios are obtained. The measurements allow to establish some trends on the behavior of the peak to peak pressure developed on the film and the power required to drive the damper when the amount of air present in the fluid film is varied. Finally, the pressure fields are analyzed to describe the effect of the variations on the amount of air present in the lubricant.

The power required to drive the damper at a constant speed was found to decrease with the amount of air on the lubricant mixture. This is an evidence of lower viscosity for the mixture with increasing amounts of air.

The maximum dynamic pressures within the squeeze film also decrease with the amount of air in the lubricant mixture. The orbit radius or eccentricity increases when the amount of air increases. This effect could be related to variations on the SFD centering force.

The presence of air on the lubricant mixture produces a zone where the squeeze film pressure remains uniform. However, this phenomenon appears only for high values of air to oil volume ratio (i.e. Mixture Quality). There is even a range of air to oil ratio where it does not appear in all the journal motion cycles. It seems to be a transition zone between one in which the no pressure variation zone never appears and one in which it appears once per cycle of journal motion.

Due to excessive pressure losses in the oil piping and instrumentation, the flow rates achieved in the tests were unmeasurable with the available instrumentation. For the same reason, it was very difficult to produce a good mixture. It is recommended to modify the test rig to obtain larger flow rates. In this way the study can be done with a quantitative evaluation of the air to oil volume ratio in order to get more reliable results, and to establish firmly the trends that appear to be present in the data obtained in this work.

Bibliography

Chamniprasart, K., Al-Sharif, A., Rajagopal, K.R., and Szeri, A. Z., **"Lubrication With Binary Mixtures: Bubbly Oil,"** Journal of Tribology, Vol. 115, April 1993, pp. 253 - 260.

Chiao-Ping Ku, Tichy, J. A., **"An Experimental and Theoretical Study of Cavitation in a Finite Submerged Squeeze Film Damper,"** Journal of Tribology, ASME, October 1990, pp. 725 - 733.

Childs, D., **"Turbomachinery Rotordynamics,"** Jhon Wiley & Sons, New York, 1993.

Einstein, A., **"Eine neue Bestimmung der Molekul-Dimension,"** Ann. Physik, 1906, Vol. 19, p. 289.

Feder, E., Bansal, P. N., Blanco, A., **"Investigation of Squeeze Film Damper Forces Produced by Circular Centered Orbits,"** Journal of Engineering for Power, Vol. 100, January 1978, pp. 15 - 21.

Hayward, A. T., **"The viscosity of Bubbly Oil,"** NE.L. Fluids Report No. 99, 1961.

Hibner, D., and Bansal, P., **"Effects of Fluid Compressibility on Viscous Damper Characteristics,"** Proceedings of the Conference on the Stability and Dynamic Response of Rotors with Squeeze Film Bearings, 1979, University of Virginia.

Humes, B., Holmes, R., **"The Role of Subatmospheric Film Pressures in the Vibration Performance of Squeeze-Film Bearings,"** Journal of Mechanical Engineering Science, vol. 20, 1978, pp. 283-289.

Jung, S. Y., **"Effects of Fluid Inertia and Cavitation on the Force Coefficients of a Squeeze Film Damper,"** Ph.D. Dissertation, Dept. Of Mechanical Eng., Texas A&M University, May 1990.

San Andres, L., Meng, G., and Yoon, S., **"Dynamic Force Response of an Open Ended Squeeze Film Damper"**, ASME paper No. 91-GT-247, 1991.

Simandiri, S., and Hahn, E. J., **"Effect of Pressurization on the Vibration Isolation capability of Squeeze Film Bearings,"** ASME, Journal of Engineering for Industry, February 1976, pp. 109-117.

Taylor, G. I., "The Viscosity of a Fluid Containing Small Drops of Another Fluid," Proc. Roy. Soc., 1932, Series A138, p. 41.

Walton, J., Walowit, E., Zorzi, E., and Schrand, J., **"Experimental Observation of Cavitating Squeeze Film Dampers,"** ASME Trans., 109, pp. 290-295 (April 1987).

Zeidan, F. Y., and Vance, J. M., **"Experimental Investigation of Cavitation Effects on The Squeeze Film Force Coefficients"**, Rotating Machinery Dynamics, DE-vol. 18-1 (1989), Asme Conference on Mechanical Vibration and Noise, pp. 237-242.

Zeidan, F. Y., and Vance, J. M., **"Cavitation Leading to a Two Phase Fluid in a Squeeze Film Damper,"** Tribology Transactions, Vol. 32 (1989), 1, 100-104.

Zeidan, F. Y., and Vance, J. M., **"Cavitation and Air Entrainment Effects on the Response of Squeeze Film Supported Rotors,"** Journal of Tribology, Vol. 112, April 1990, pp. 347 - 353.

Zeidan, F. Y., and Vance, J. M., **"A Density Correlation for a Two-Phase Lubricant and its Effect on the Pressure Distribution,"** Tribology Transactions, Vol. 33, 1990, pp. 641 - 647.

Table 1: Measurements Set # 1

Case	Speed [RPM]	Voltage [Volt]	Current [amp]	T air inlet [C]	T mix in [C]	T mix film [C]	T mix out [C]	P oil inlet [bar]	P air inlet [bar]	P mix inlet [bar]	Mixture Quality
1	1000	6.3	56	18.9	27.2	27.2	26.7	3.4	2.7	2.7	0
2	1000	6.1	55	19.4	26.7	28.9	28.9	3.1	2.7	2.4	10
3	1000	6.1	53	18.9	26.7	28.3	28.3	3.2	2.7	2.4	30
4	1000	5.9	54	18.9	26.7	28.3	28.3	3.2	2.7	2.4	50

Case	P z1 min [bar]	P z1 max [bar]	P z2 min [bar]	P z2 max [bar]	h min [10^-4 m]	h max [10^-4 m]
1	-1.544	3.320	-1.575	2.685	1.844	5.046
2	-1.486	3.134	-1.496	2.589	1.797	5.076
3	-1.523	3.241	-1.443	2.619	1.701	5.171
4	-1.496	3.375	-1.430	2.712	1.618	5.243

Case	Mixture Quality	Power [Wats]	Delta P [bars]	Dimlss. Orbit R.	Normal. Delta P
1	0	352.8	4.215	0.464	9.084
2	10	335.5	4.026	0.475	8.481
3	30	323.3	3.875	0.484	8.013
4	50	318.6	3.808	0.507	7.518

Table 2: Measurements Set # 2

Case	Speed [RPM]	Voltage [Volt]	Current [amp]	T air inlet [C]	T mix in [C]	T mix film [C]	T mix out [C]	P oil inlet [bar]	P air inlet [bar]	P mix inlet [bar]	Mixture Quality
1	1000	6.3	53	18.3	25.6	27.2	27.8	3.1	2.7	2.1	0
2	1000	6.1	52	18.9	26.7	28.9	28.9	3.1	2.7	2.1	10
3	1000	6.0	51	18.9	26.7	29.4	29.4	3.1	2.7	2.1	30
4	1000	5.9	49	18.9	26.7	29.4	30	3.1	2.7	2.4	50

Case	P z1 min [bar]	P z1 max [bar]	P z2 min [bar]	P z2 max [bar]	h min [10^-4 m]	h max [10^-4 m]
1	-1.543	3.340	-1.535	2.757	1.803	5.087
2	-1.492	3.319	-1.436	2.724	1.726	5.254
3	-1.482	3.182	-1.419	2.645	1.666	5.212
4	-1.471	3.306	-1.406	2.731	1.649	5.379

Case	Mixture Quality	Power [Wats]	Delta P [bars]	Dimlss. Orbit R.	Normal. Delta P
1	0	333.9	4.247	0.476	8.924
2	10	317.2	4.101	0.503	8.159
3	30	306.0	3.877	0.495	7.837
4	50	289.1	3.803	0.522	7.288

Table 3: Measurement Fluctuations Set #1

Delta Pressure [bar]

Case	Mix. Qty.	Ave.	max	%	Min	%
1	0	4.2154	4.26	+1.06	4.149	-1.58
2	10	4.026	4.085	+1.47	3.953	-1.81
3	30	3.875	4.062	+4.83	3.594	-7.25
4	50	3.808	4.142	+8.77	3.243	-14.84

Non Dimensional Orbit Radius (e/c)

Case	Mix. Qty.	Ave.	max	%	Min	%
1	0	0.464	0.467	+0.59	0.462	-0.48
2	10	0.475	0.478	+0.69	0.472	-0.57
3	30	0.484	0.506	+4.59	0.469	-3.12
4	50	0.507	0.528	+4.33	0.488	-3.56

Normalized Delta Pressure

Case	Mix. Qty.	Ave.	Max.	%	Min.	%
1	0	9.084	9.181	+1.06	8.941	-1.58
2	10	8.481	8.605	+1.47	8.327	-1.81
3	30	8.013	8.399	+4.83	7.432	-7.25
4	50	7.518	8.178	+8.77	6.403	-14.84

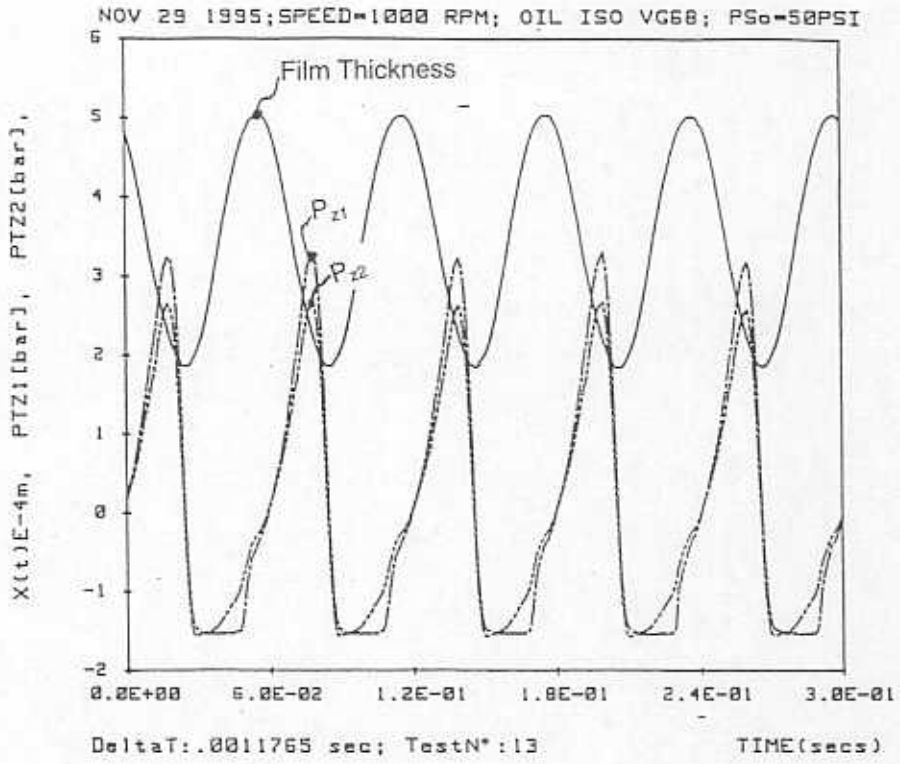

Fig. 4 a.- Pressure Field and Film Thickness - Case 1 of set 1 (Mixture Quality 0)

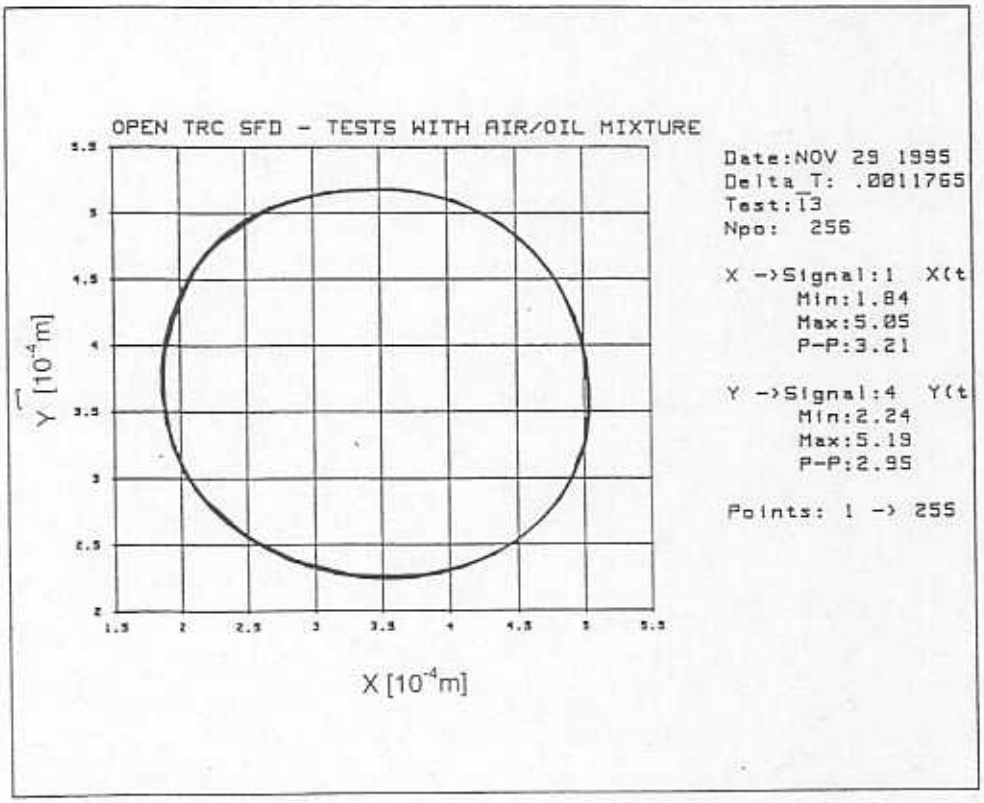

Fig. 4 b.- Journal Center Orbit - Case 1 of set 1 (Mixture Quality 0)

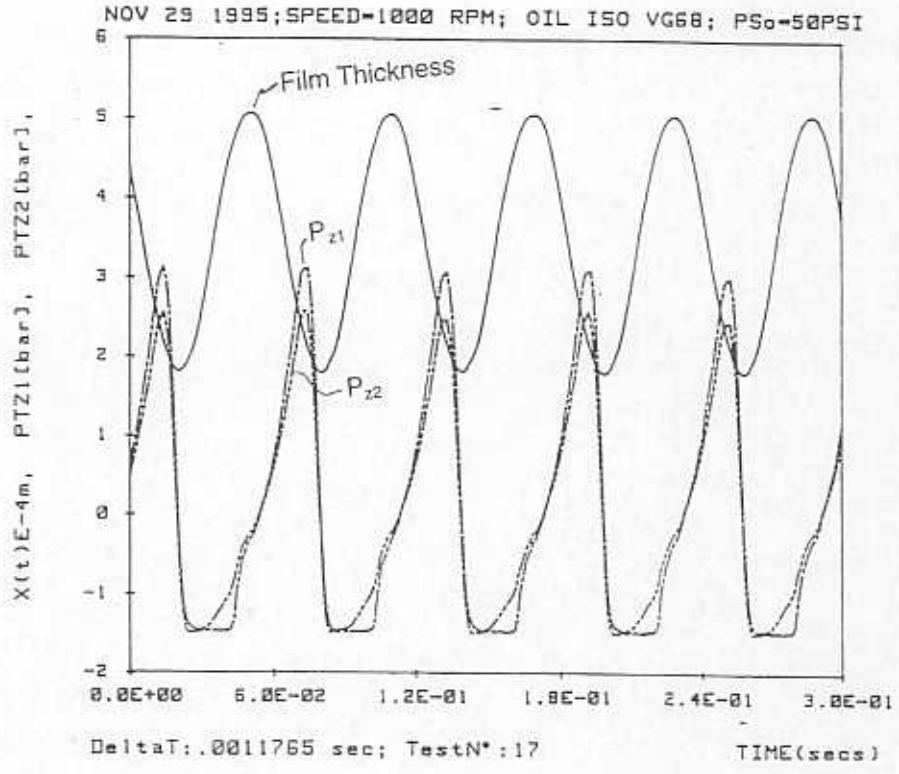

Fig. 5 a.- Pressure Field and Film Thickness - Case 2 of set 1 (Mixture Quality 10)

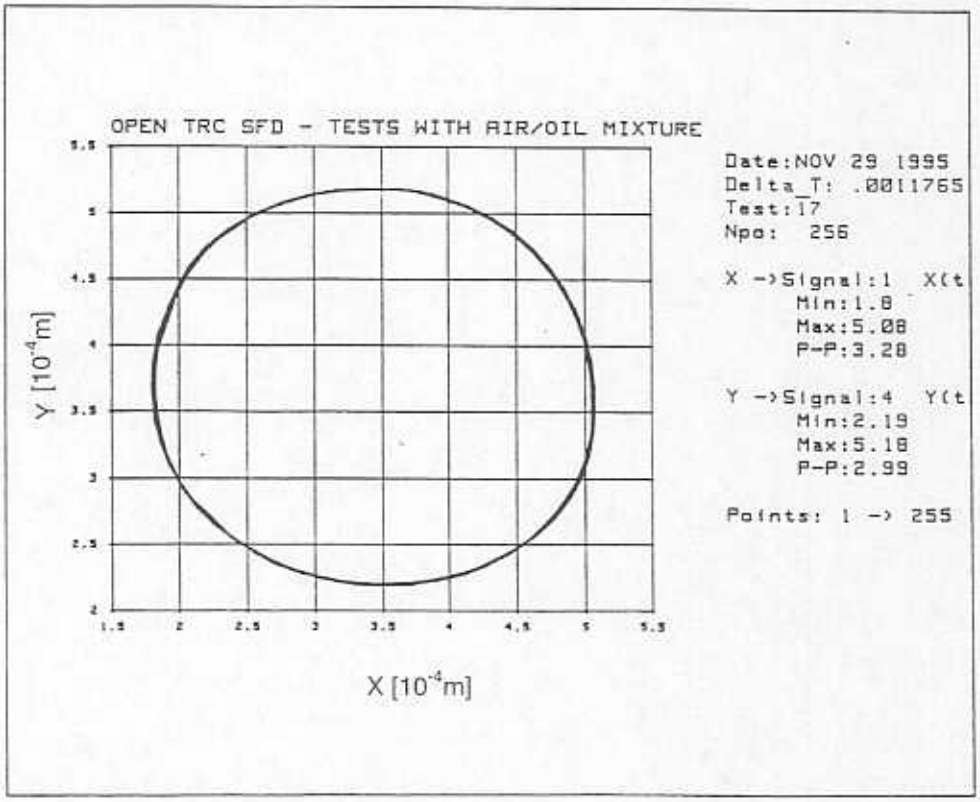

Fig. 5 b.- Journal Center Orbit - Case 2 of set 1 (Mixture Quality 10)

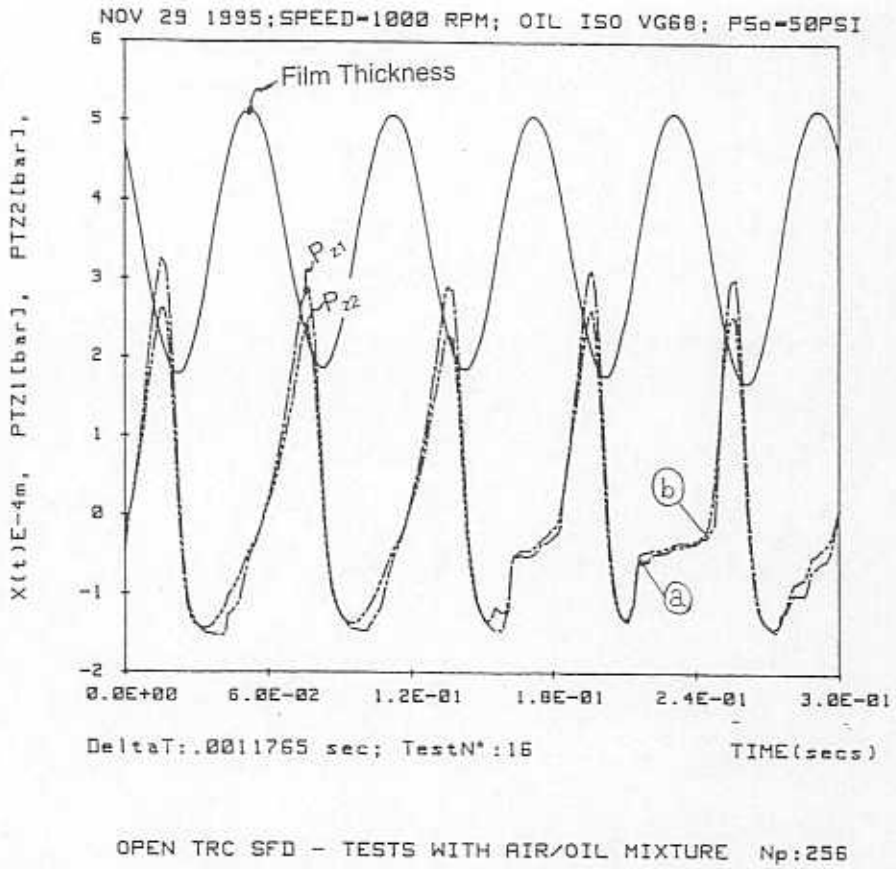

Fig. 6 a.- Pressure Field and Film Thickness - Case 3 of set 1 (Mixture Quality 30)

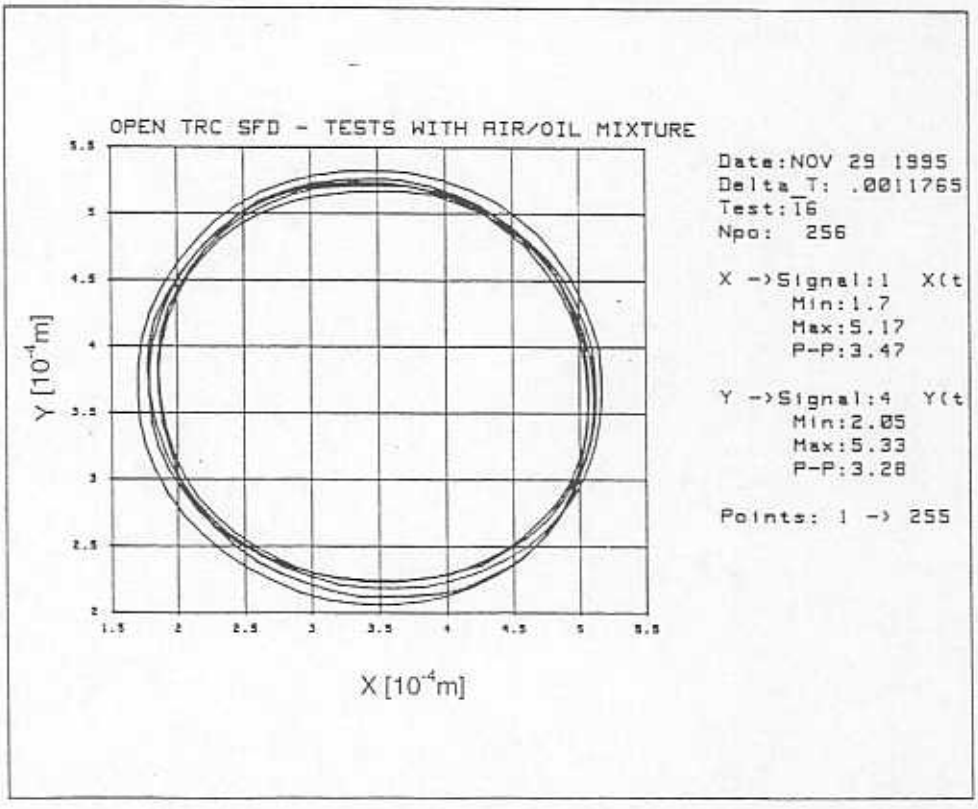

Fig. 6 b.- Journal Center Orbit - Case 3 of set 1 (Mixture Quality 30)

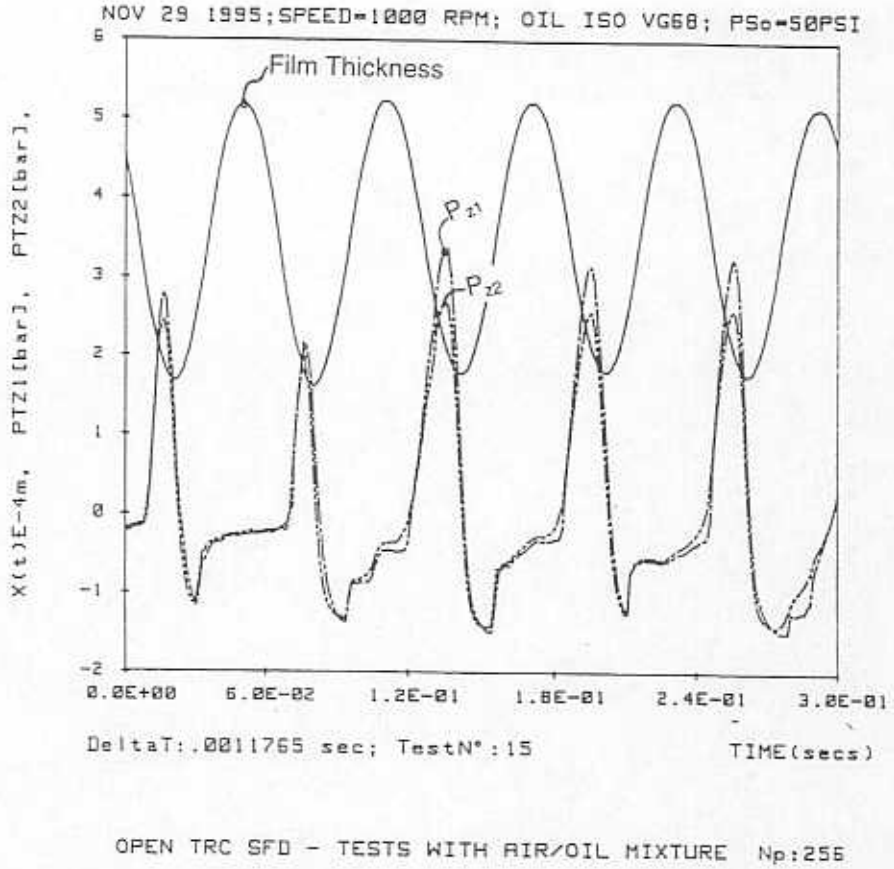

Fig. 7 a.- Pressure Field and Film Thickness - Case 4 of set 1 (Mixture Quality 50)

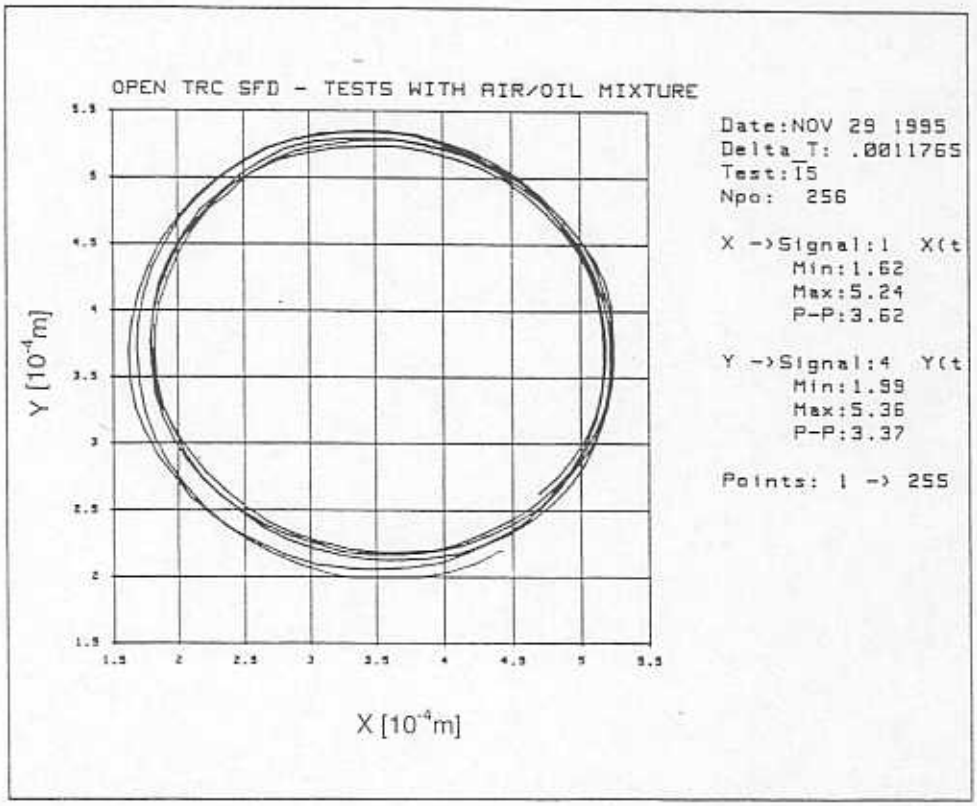

Fig. 7 b.- Journal Center Orbit - Case 4 of set 1 (Mixture Quality 50)

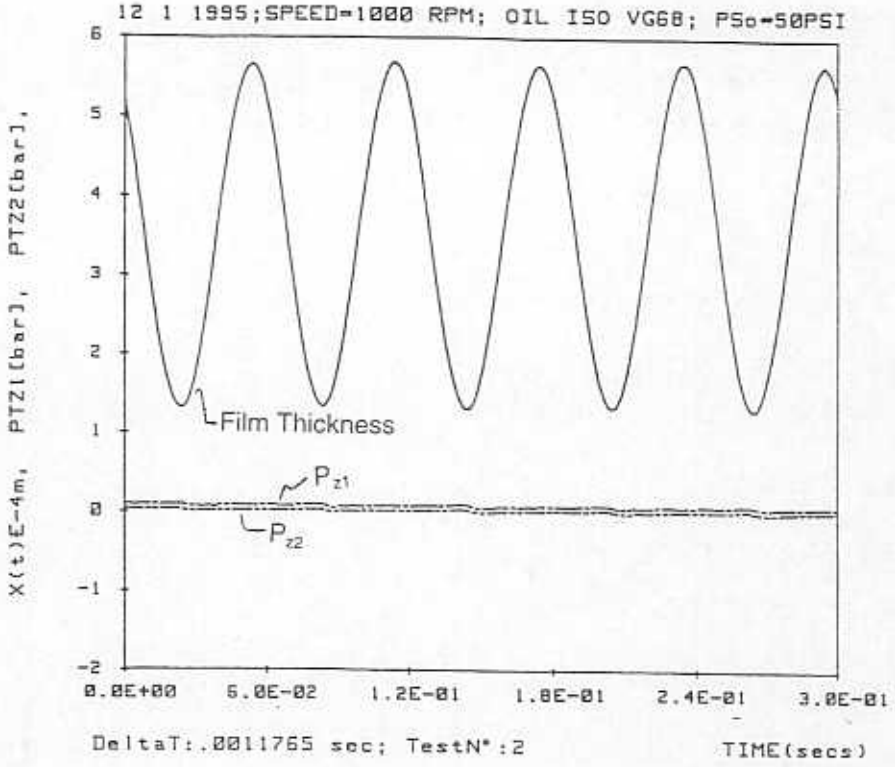

Fig. 8 a.- Pressure Field and Film Thickness - No oil

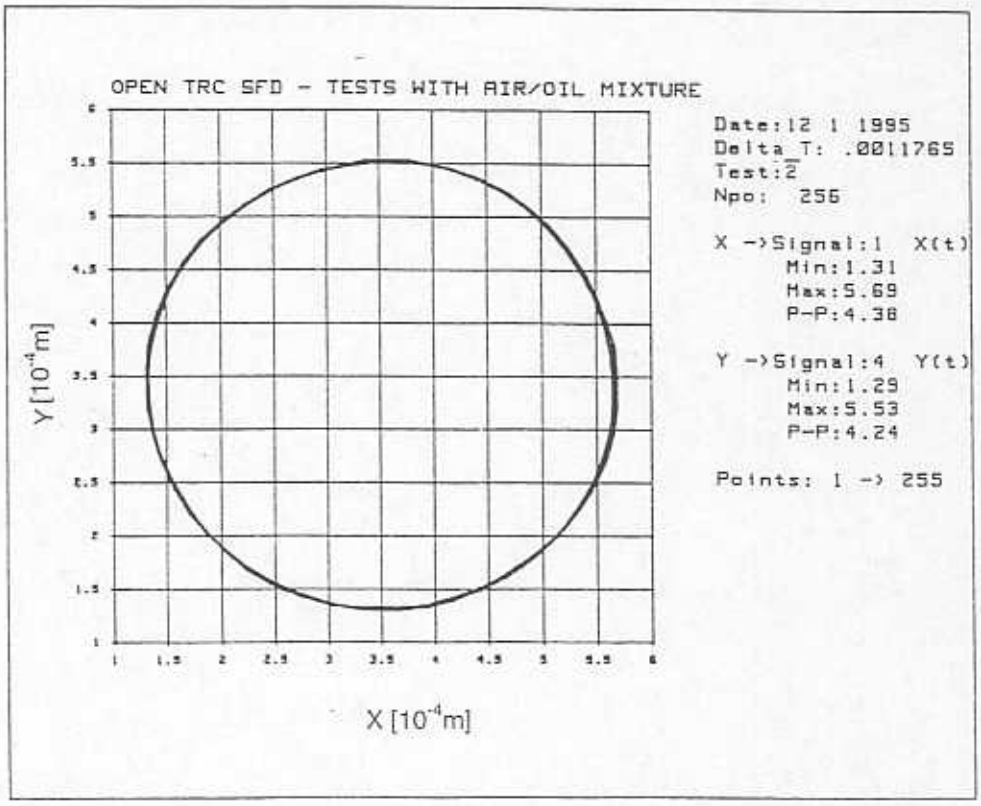

Fig. 8 b.- Journal Center Orbit - No oil

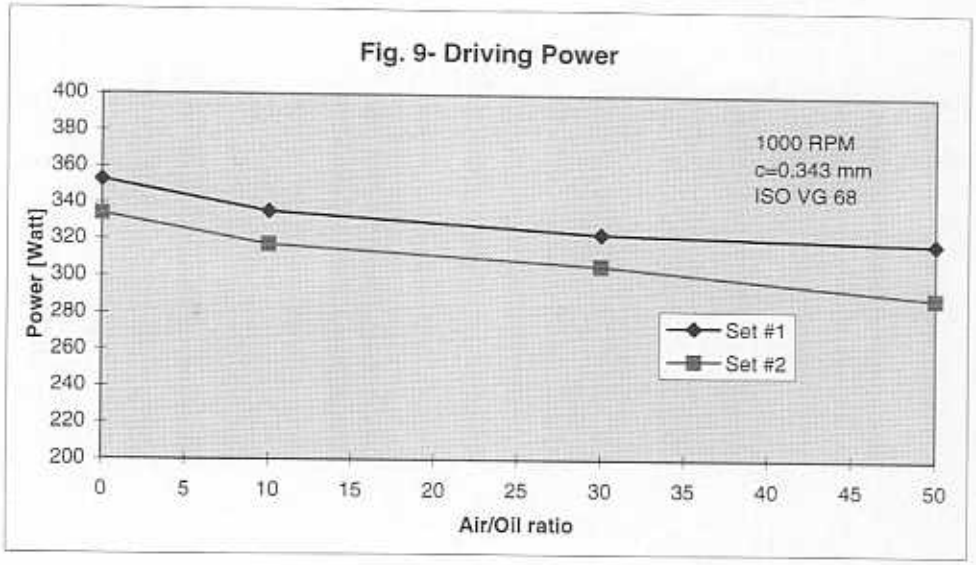
Fig. 9- Driving Power
Power [Watt]
400
380
360
340
320
300
280
260
240
220
200
0
5
10
15
20
25
30
35
40
45
50
Air/Oil ratio
1000 RPM
c=0.343 mm
ISO VG 68
Set #1
Set #2

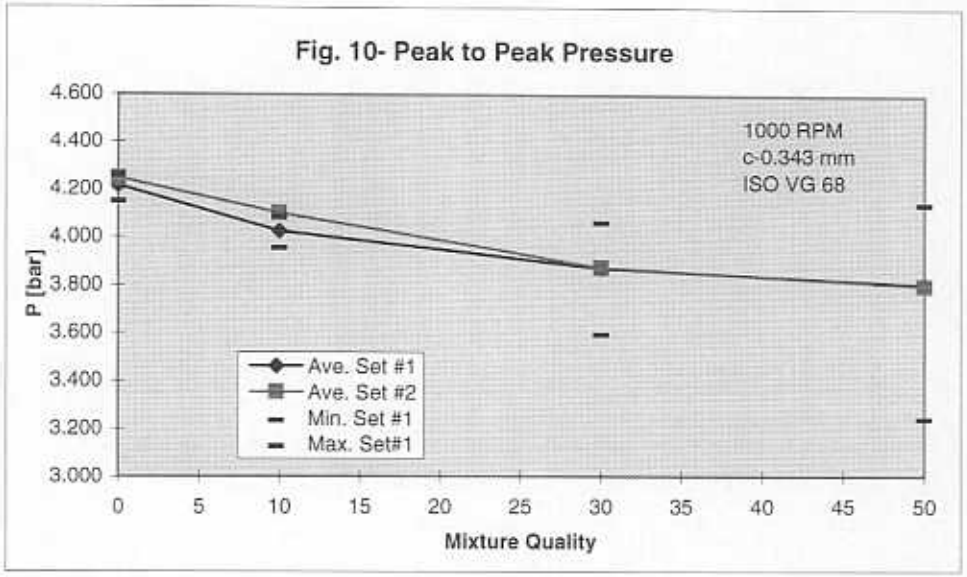
Fig. 10- Peak to Peak Pressure
P [bar]
4.600
4.400
4.200
4.000
3.800
3.600
3.400
3.200
3.000
0
5
10
15
20
25
30
35
40
45
50
Mixture Quality
1000 RPM
c-0.343 mm
ISO VG 68
Ave. Set #1
Ave. Set #2
Min. Set #1
Max. Set#1

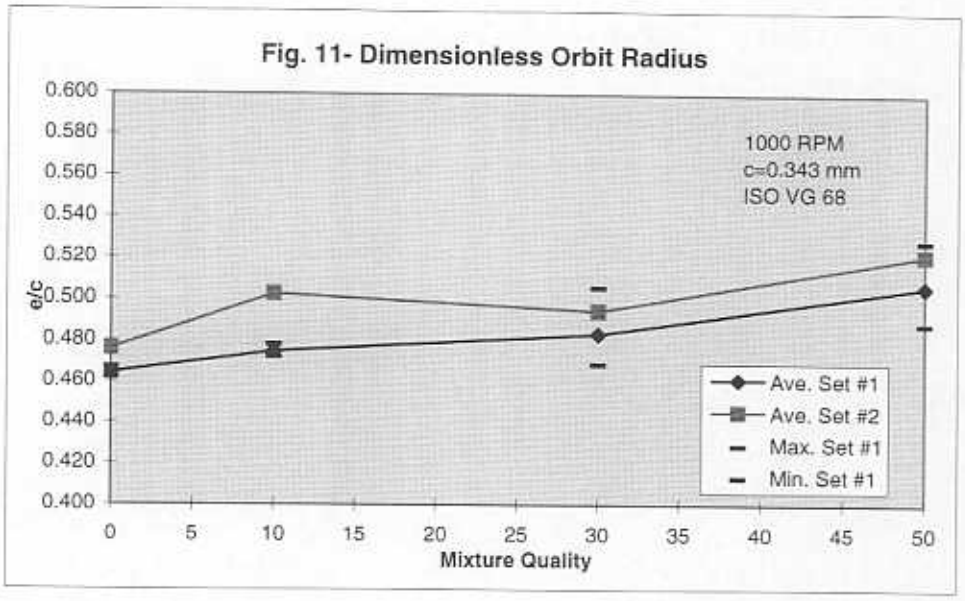
Fig. 11- Dimensionless Orbit Radius
0.600
0.580
0.560
0.540
0.520
0.500
0.480
0.460
0.440
0.420
0.400
e/c
1000 RPM
c=0.343 mm
ISO VG 68
Ave. Set #1
Ave. Set #2
Max. Set #1
Min. Set #1
0
5
10
15
20
25
30
35
40
45
50
Mixture Quality

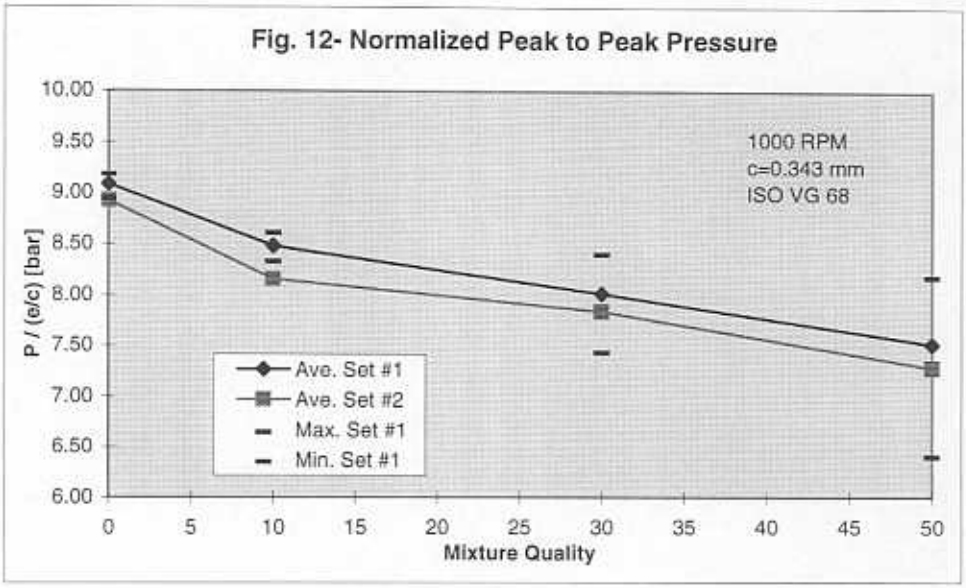
Fig. 12- Normalized Peak to Peak Pressure
10.00
9.50
9.00
8.50
8.00
7.50
7.00
6.50
6.00
P / (e/c) [bar]
1000 RPM
c=0.343 mm
ISO VG 68
Ave. Set #1
Ave. Set #2
Max. Set #1
Min. Set #1
0
5
10
15
20
25
30
35
40
45
50
Mixture Quality